New Phytologist

Variations of vessel diameter and $\delta^{13}C$ in false rings of *Arbutus unedo* L. reflect different environmental conditions

Giovanna Battipaglia[1,2], Veronica De Micco[3], Willi A. Brand[4], Petra Linke[4], Giovanna Aronne[3], Matthias Saurer[5] and Paolo Cherubini[1]

[1]WSL Swiss Federal Institute for Forest, Snow and Landscape Research, CH-8903 Birmensdorf, Switzerland; [2]ENEA, Italian National Agency for New Technologies, Energy and Sustainable Economic Development, Via Anguillarese 301, I-00123 Rome, Italy; [3]Department of Arboriculture, Botany and Plant Pathology, University of Naples Federico II, via Università 100, I-80055 Portici (Naples), Italy; [4]Max Plank Institute for Biogeochemistry, Box 100164, D-07701, Jena, Germany; [5]Paul Scherrer Institute, CH-5232 Villigen, Switzerland

Author for correspondence:
Giovanna Battipaglia
Tel: +39 0630483598
Email: giovanna.battipaglia@enea.it

Received: *7 July 2010*
Accepted: *16 July 2010*

New Phytologist (2010) **188**: 1099–1112
doi: 10.1111/j.1469-8137.2010.03443.x

Key words: *Arbutus unedo,* carbon isotopes, dendrochronology, intra-annual density fluctuations, Mediterranean ecosystems, quantitative wood anatomy.

Summary

- Woody species in Mediterranean ecosystems form intra-annual density fluctuations (IADFs) in tree rings in response to changes in environmental conditions, especially water availability.
- Dendrochronology, quantitative wood anatomy and high-resolution isotopic analysis (using a laser ablation technique) were used to characterize IADFs in *Arbutus unedo* shrubs grown on two sites with different water availability on the island of Elba (Italy).
- Our findings show that IADF characterization can provide information about the relationship between environmental factors and tree growth at the seasonal level. At the more xeric site, IADFs mainly located in the early and middle parts of the annual ring, showed a decrease in vessel size and an increase in $\delta^{13}C$ as a result of drought deficit. Opposite trends were found at the more mesic site, with IADFs located at the end of the ring and associated with a lower $\delta^{13}C$. Moreover, at the first site, IADFs are induced by drought deficit, while at the second site IADFs are linked with the regrowth in the last part of the growing season triggered by favourable wet conditions.
- This combined approach is a promising way for dating problematic wood samples and interpreting the phenomena that trigger the formation of IADFs in the Mediterranean environment.

Introduction

Water availability is the key factor driving ecophysiological processes in Mediterranean species, influencing photosynthetic rates, cambial activity, dry matter production, allocation of carbon to roots and the primary and secondary growth of woody plants (Margaris & Papadogianni, 1977; Peñuelas, 1996; Salleo *et al.*, 1997). According to the Intergovernmental Panel on Climate Change (IPCC, 2007) report, longer and more severe drought periods are expected in Mediterranean ecosystems in the near future. To cope with drought conditions, Mediterranean trees have evolved phenological, physiological and morphological adaptations (Baas, 1976; Jacobsen *et al.*, 2007a,b; De Micco *et al.*, 2008), which often result in specific patterns of cambial activity leading to intra-annual density fluctuations (IADFs) in the wood, also referred to as 'false rings' or 'double rings'. IADFs are caused by the interruption of the normal course of growth during the growing season, thus determining a zone of wood characterized by an abrupt change in wood density (Tingley, 1937; Schulman, 1938). In Mediterranean-type ecosystems, IADFs occur irregularly in both space (at different sites in the same year) and time (in different years at the same site), as well as species and individual trees (Cherubini *et al.*, 2003). This makes it difficult to study tree rings and analyse the relationships between environmental factors and wood formation during tree growth.

Intra-annual density fluctuations have been frequently described in temperate and Mediterranean trees, but the actual ecophysiological processes behind their formation remain unclear, although several hypotheses have been explored (Glerum, 1970; Campelo *et al.*, 2007; De Micco *et al.*, 2007; Vieira *et al.*, 2009). Kuo & McGinnes (1973) speculated that false ring formation in *Juniperus virginiana* L. may be governed by changes in hormonal concentrations and increased water stress. Rigling *et al.* (2001) found IADFs in *Pinus sylvestris* L. useful to distinguish between different ecological sites characterized by different substrate types and climatic conditions, especially drought stress. In a subsequent study, Rigling *et al.* (2002) found that seasonal variations in temperature and precipitation produced IADFs with variations not only in their occurrence across sites, but also in their position within the ring.

Anatomical differences in lumen size and the shape of tracheids, as well as differences in the stable carbon isotopic composition of IADFs were identified in *Pinus pinaster* Aiton by De Micco *et al.* (2007) and in spruce and pine trees by Vaganov *et al.* (2009), confirming that wood anatomy and the isotope composition of tree rings may serve as a useful parameter to expand the possibilities of interpreting IADFs in relation to physiological and ecological processes. In particular the $^{13}C : ^{12}C$ ratio of tree-ring wood reflects water availability (Farquhar & Richards, 1984), soil water content (Panek & Goldstein, 2001), water-use efficiency (Matzner *et al.*, 2001; Ponton *et al.*, 2001) or xylem hydraulic properties (Panek, 1996). Trees respond to limited water resources, particularly when low precipitation is accompanied by relatively warm conditions, as during the Mediterranean summer, by reducing the stomatal conductance and photosynthetic rate. This results in a change in the isotope fractionation during CO_2 uptake and fixation in the leaves, and subsequent carbon isotope composition of the organic matter (Scheidegger *et al.*, 2000).

Most studies on the impact of climate on isotope composition and wood anatomy of tree rings have focused on trees, mainly conifers. However, in Mediterranean ecosystems, shrubs are dominant in maquis and garrigue formations where trees cannot survive. Shrub form seems to be an adaptation based on the strategy of forming relatively small, low-risk, 'low-investment' stems that can be easily sacrificed in areas characterized by severe environmental stress (Rundel, 1991; Wilson, 1995). In Mediterranean ecosystems, peculiar anatomical traits of shrub wood are responsible for species' ability to withstand fluctuations in water availability and vary considerably between and within plants (Carlquist, 1975; Correia *et al.*, 1987; Baas *et al.*, 2004; De Micco *et al.*, 2006, 2008). This phenomenon suggests that shrubs are very plastic and can thus be considered sensitive models for studying intra-annual variations in properties of Mediterranean woods in relation to changing climatic conditions.

In this paper, we focus on *Arbutus unedo* L., a common species in the Mediterranean maquis, which can grow as a shrub or small tree. Its growth is severely influenced by climatic condition and water availability (Maltez-Mouro *et al.*, 2007; Ogaya & Peñuelas, 2008). We investigated the climate sensitivity of this species by analysing the relationships between climate, mainly via water availability, and IADFs. The specific aims of this study were to describe the occurrence and type of IADFs under different environmental conditions; to analyse the variation in vessel size and carbon isotope composition along the rings with and without IADFs; and to determine how the formation of IADFs is influenced by climate. To pursue these aims, we used a novel multidisciplinary approach combining dendroecology, intra-annual laser-ablation isotopic analysis and quantitative wood anatomy (QWA).

Materials and Methods

Study area

We selected two study sites on Isola d'Elba, an island in the Tyrrhenian sea (Italy). The sites are characterized by different amounts of soil moisture (*c.* 40% difference) and different soil depths (*c.* 20% difference). Both sites are dominated by evergreen shrub species, including *Arbutus unedo* L., *Erica arborea* L. and *Cistus salvifolius* L., with scattered *Quercus ilex* L. and *Pinus pinaster* Aiton. However, the first site (ME), located in the Nivera Valley at 460 m above sea level (asl; 42°46′N, 10°11′E) presents more mesic species (such as *Ostrya carpinifolia* Scop., *Osmunda regalis* L.) growing as trees in comparison to the second site (XE), located on Monte Perone at 420 m asl (42°46′N, 10°12′E), where the vegetation was more open and scattered, characterized by a higher frequency of more xeric species and shrub forms (such as *Cistus monspeliensis* L., *C. salvifolius* L. and *Inula viscosa* L. Ait.). Precipitation and temperature data were not easily accessible and were obtained from the Portoferraio meteorological station located *c.* 10 km from the sites (42°49′N, 10°20′E, 25 m asl). We also used precipitation data from the nearby stations of Monte Perone (42°46′N, 10°12′E 250 m asl) and Pianosa Island (42°35′N, 10°06′E, 15 m asl) to describe the evolution of rainfall in the area during the period 1990–2008. The average summer and winter temperatures were 23.4 and 9.4°C, respectively, while precipitation was mainly concentrated in autumn and winter, with an average of 375 mm during the period 1970–2007 (Fig. 1c).

Soil samples

At each site, 10 soil cores, 5 cm deep, were sampled, after litter removal, during the spring/summer season. Samples were put into polythene bags and mixed. In the laboratory, stones, large roots and other coarse fragments were removed

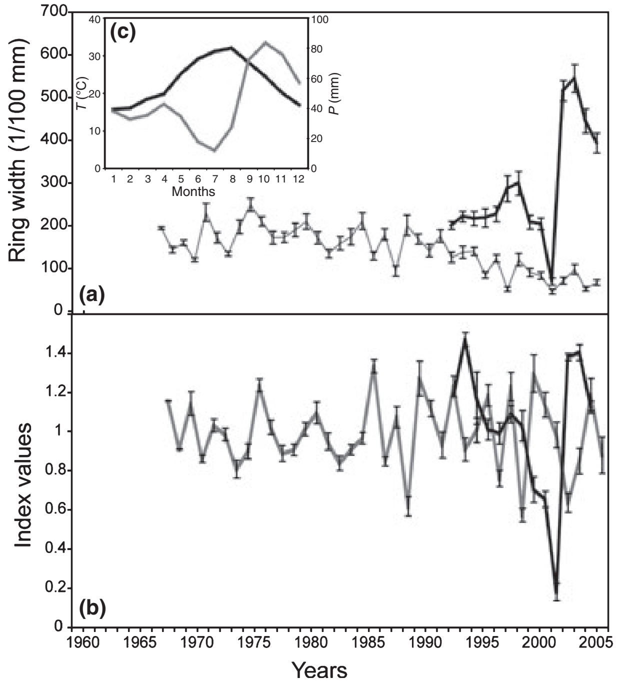

Fig. 1 Average ring-width chronology with standard deviation (SD) for the ME site (grey) and for the XE site (black) using either raw data (a) or data after detrending (b). (c) Mean annual temperature (black) and mean annual precipitation (grey line) recorded in Elba during the period 1970–2007.

using a 2 mm sieve. The sieved soil was stored at 5°C. Preliminary analyses were carried out, including water-holding capacity (WHC), moisture and pH, following the standard procedures (USDA, Natural Resources Conservation Service, National Soil Survey Center, 1996).

Tree-ring data, chronology development and microscopy

Small trees (3–5 m height, 5–10 cm diameter) were sampled. Multistem plants were avoided. A total of 10 *A. unedo* plants were cut at both sites, and three disks from the base of each shrub were cut and air-dried.

Standard dendrochronology typically involves sampling 10–20 trees per site to capture the site signal and to produce a climate reconstruction. However, our sites were in the National Park of the Tuscan Archipelago and we were allowed to sample the minimum number of specimens to get reliable chronologies, useful for our aims. Signal strength of the chronologies was assessed using the 'expressed population signal' (EPS; Wigley *et al.*, 1984). EPS is an absolute measure of chronology error that determines how well a chronology, based on a finite number of trees, estimates the theoretical population chronology from which it has been drawn. EPS quantifies the degree to which each particular sample chronology portrays the theoretical population chronology.

Intra-annual density fluctuations were identified on each disk and each disk was cross-sectioned with a sliding microtome. Sections (15 μm thick) were stained with safranin and astra blue, dehydrated through an ethanol series, immersed with xylol and mounted on slides with Canada Balsam (Schweingruber, 1978; Gärtner *et al.*, 2001).

The microsections were studied under a light microscope (Olympus BH-2, Hamburg, Germany), equipped with a photo-microadapter (Olympus OM-Mount) and a camera (Olympus OM101). The microphotographs were digitized and calibrated to identify the IADFs. Signs of IADFs were the presence of collapsed or crushed xylem elements along the ring, often lacking lignin as reported by Cherubini *et al.* (2003). Moreover, IADFs were often not uniformly present along the circumference of an annual tree ring and could be distinguished by the sharp boundary of the real rings. In addition, all samples were visually cross-dated (Stokes & Smiley, 1968). The procedure was time-consuming but allowed a precise identification of IADFs.

The occurrence and position of IADFs within the annual rings were recorded. The IADFs were classified according to their position as follows: type 1, located at the beginning of the annual ring (early-IADF); type II, located in the middle of the annual ring (middle-IADF); type III, located at the end of the ring (late-IADF) (Fig. 2). Most IADFs found in plants growing in the XE site were classified as early-IADFs, while late-IADFs were the most frequent in the ME site.

After the identification of IADFs, the tree-ring width was measured using a LINTAB linear table and a micrometer with a resolution of 0.01 mm. The program COFECHA (Holmes, 1983) was run to validate the cross-dating and measurements and to find potential errors. Once all measurement series had been validated, tree-ring chronologies were developed. Series were detrended to remove long-term growth trends embedded in the raw tree-ring series, which were thought to be induced by nonclimatic influences, such as ageing and competition between trees (Fritts, 1976). Tree-ring indices were calculated as residuals from the estimated age trend. The new dataset was used for all the statistical analyses. Several descriptive statistics, commonly used in dendrochronology, were computed to compare site chronologies.

These included the standard deviation (SD), which estimates the variability of measurements for the whole series, and the mean sensitivity (MS), which is an indicator of the mean relative change between consecutive ring widths and is calculated as the absolute difference between consecutive indices divided by their mean value.

Analysis of IADFs

The frequency of IADFs yr^{-1} was calculated as:

$$F = N/n$$

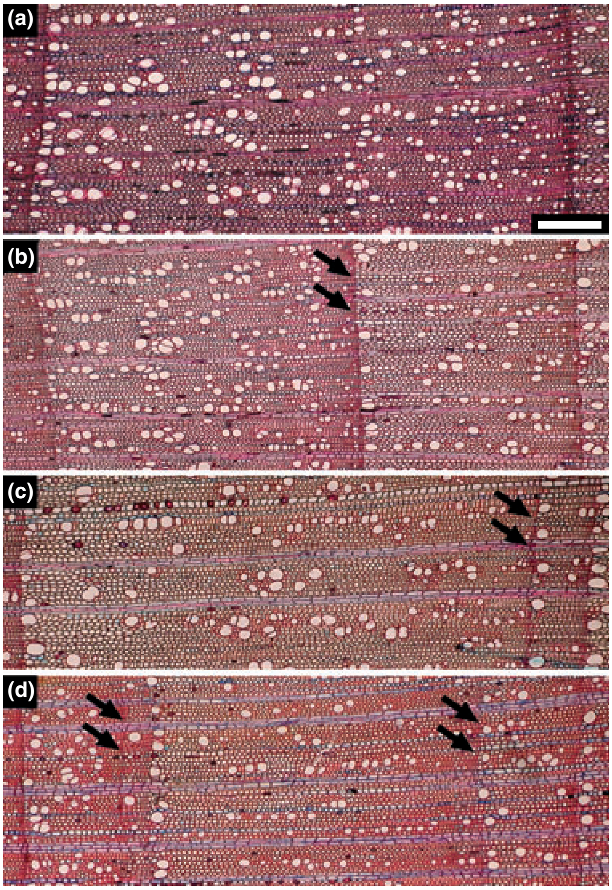

Fig. 2 Microphotographs of wood cross-sections of *Arbutus unedo* showing rings with and without intra-annual density fluctuations (IADFs): (a) ring without IADFs (XE site); (b) ring with a middle-IADF (type 2; XE site); (c) ring with a late-IADF (type 3; ME site); (d) ring with an early- and a late-IADF (types 1 and 3; ME site). Cambium is on the right side. Images are all at the same magnification: bar, 100 μm.

[correction added after online publication 28 September 2010: the equation was corrected to F = N/n] where N is the number of trees presenting IADFs in a given year, and n is the total number of trees sampled that year. The difference in the sampling size was adjusted using the method proposed by Osborn *et al.* (1997) for ring-width chronologies by calculating:

$$f = Fn^{0.5}$$

where f is the stabilized IADF frequency.

Statistical analyses were carried out with ANOVA, using SYSTAT (Systat Software Inc., Chicago, IL, USA). To determine the association between climate, tree-ring chronologies and IADF frequency, we used Pearson's and Spearman's correlation coefficients and compared the populations of the two sites over the same overlapping period.

Quantitative wood anatomy

The microsections of *A. unedo* were observed by means of a transmitted light microscope (BX60; Olympus) in order to select 10 tree rings with IADFs and 10 without IADFs for each site. Tree rings showing middle-IADFs (type 2) were selected for the XE site, while rings with late-IADFs (type 3) were chosen from the ME site. Microphotographs including the whole tree-ring width were taken in three different regions along the circumference with a digital camera (CAMEDIA C4040; Olympus). The images were analysed with AnalySIS 3.2 (Olympus) to quantify the anatomical features. In each microphotograph, a transect, 150–200 μm wide, throughout the ring width, was selected. Along each transect, the lumen area was measured in all vessel elements encountered moving from the outside border of the tree ring (beginning of earlywood, EW) towards the inside ring boundary (ending of latewood, LW). In the resulting data series, the progressive number of each measured vessel was standardized according to distance from the earlywood border, with the whole ring width being considered equal to 100%. Subsequently, each vessel was characterized by two coordinates: *Y*, corresponding to its lumen area; and *X*, corresponding to the distance from the beginning of the ring, expressed as a percentage. These coordinates were plotted into dispersion graphs. The result was a sort of chronology of vessel size comparable to the chronologies of tree-ring width commonly used in traditional dendrochronology. Having ascertained that, in all samples, the distribution of vessel size was similar in the three transects considered in each ring, the data measured in the three transects were pooled together in order to compare the shape of the resulting chronologies between rings with and without IADFs and between the two sites.

Finally, the data from all rings with IADFs and those from rings without IADFs were pooled together for each site to obtain four series of data; simple moving average and interpolation equations were then calculated.

Carbon isotopes

The same tree rings as those selected for anatomical analysis were used for the analysis of stable carbon isotopes. Since we had three disks for each tree, we had enough material to divide each ring into 1 yr intervals and then proceed with a further subdivision for selected rings. The tree rings with IADFs were split (under a dissection microscope, with a razor blade) into three sections from pith to bark: EW, IADFs and LW. Each section was milled with a centrifugal mill (Retsch, Hann, Germany), and an aliquot of a few mg was packed in porous bags and used for cellulose extraction (Battipaglia *et al.*, 2008). $\delta^{13}C$ values were determined using an elemental analyser linked to an isotopic ratio mass spectrometer (Thermo-Fisher, Bremen, Germany) via a variable open split interface (Conflo II, Finnigan Mat, Bremen, Germany).

Isotope ratio deviation results are presented in the common δ notation:

$$\delta^{13}\mathrm{C} = [(^{13}R_{\mathrm{sa}}/^{13}R_{\mathrm{ref}}) - 1],$$

with δ-values expressed in per mill (‰) on the international VPDB (Vienna Pee Dee Belemnite) scale for carbon-13. ^{13}R refers to the number ratio of ^{13}C to ^{12}C isotopes in the sample ('sa') and the reference ('ref'), respectively.

δ^{13}C for the 4 yr period 2004–2007 were also determined on a laser ablation–combustion line (LA-C-GC_IRMS, Nd-YAG 266 nm UV laser; Merchantek–New Wave, Fremont, CA, USA) coupled online to an isotope ratio mass spectrometer (Thermo-Finnigan Delta$^+$ XL, Thermo Fisher Scientific Inc., San Jose, CA, USA) using a home-made combustion/open-split interface, as described by Schulze *et al.* (2004). The exact location of each ablation spot was visualized with a camera mounted directly on the laser ablation station. The distance between the laser shots is *c.* 150 μm, and the series of shots were repeated radially along the same line.

The data provided in Francey *et al.* (1999) and McCarroll & Loader (2004) were used to remove the atmospheric δ^{13}C trend from the carbon isotope data series. The corrected series were then employed in all the statistical analyses.

Results

Tree – ring width

Ring-width chronologies are presented in Fig. 1. The 10 trees have a similar age in each site. The total time span of the chronologies extended from 1992 to 2007 for the trees at the XE site (grey line) and from 1970 to 2007 for those at the ME site (black line).

For the samples from the XE site, the measured cores had a mean sensitivity of 0.479, whereas those from the ME site had a mean sensitivity of 0.432. For both chronologies, the EPS was above the critical value of 0.85, indicating a strong common signal. Although the presence of several IADFs hampered the identification of the rings and hindered the dating, it was still possible to measure and cross-date the rings, using pointer years. At the XE site, there was one particularly narrow pointer year (2003) in all the samples, whereas at the ME site, 1984, 1990 and 1999 were narrow rings in all samples.

The variability between individuals of the same site was high, probably as a consequence of competition processes for water, nutrients and other resources. The difference in growth between the trees of the two sites was also significant, with a mean growth ring width of 146 ± 51 × 10^{-2} mm for trees at the ME site and a mean growth rate of 281 ± 138 × 10^{-2} mm for trees at the XE site.

The correlation analyses (Table 1) identified several significant relationships between tree- ring growth and climate (temperature and precipitation). At the XE site, the tree-ring width was negatively correlated with the April and May temperatures ($r = -0.38$, $P < 0.05$) and positively correlated with the March and September temperatures ($r = 0.41$, $P < 0.05$). There was no significant influence of precipitation on ring width. At the ME site, precipitation in the period June–September influenced tree-ring growth positively ($r = 0.60$, $P < 0.001$), while temperature had a significant effect only in March ($r = 0.54$, $P < 0.01$).

Table 1 Correlation coefficients between climatic factors (CFs, temperature and precipitation), tree-ring width (TRW) and intra-annual density fluctuations (IADFs) are shown

Site	Parameters	CF	Months	*r*
XE	TRW	t	AM	−0.38*
XE	TRW	t	M–S	0.41*
ME	TRW	p	J–S	0.60***
ME	TRW	t	March	0.54**
XE	IADFs	t	MA	0.52**
ME	IADFs	p	JJAS	0.62**
XE	δ^{13}C IADF	p	AM	−0.44*
ME	δ^{13}C IADF	p	AS	0.86***
XE	δ^{13}C EW	t	MA	0.59***
XE	δ^{13}C EW	p	MA	−0.48**
ME	δ^{13}C EW	p	MAM	−0.78**
XE	δ^{13}C LW	t	O	0.70***
XE	δ^{13}C LW	p	JJA	−0.74***
ME	δ^{13}C LW	p	ASO	−0.98***

Significance levels according to Student's *t*-test: *, $P < 0.05$; **, $P < 0.01$; ***, $P < 0.001$.

t, temperature; p, precipitation; AM, April, May; MS, March–September; JS, June–September; MA, March, April; JJAS, June, July, August, September; AS, August, September; MAM, March, April, May; O, October; JJA, June, July, August; ASO, August, September, October.

IADFs

The IADF-stabilized frequency distribution in relation to calendar years is shown in Fig. 3(a). In order to compare the two sites better, we analysed only the common period for which data were available at both sites (1994–2006). The shrubs at the XE site appeared to be more prone to false ring formation ($f = 1.2$) than those at the ME site ($f = 0.5$).

During some years, only the trees growing at one site formed IADFs, while in other years (1982–1983) none did. In 2004, *A. unedo* presented IADFs only at the XE site, while in 2002 and 2003, IADFs were formed only at the ME site.

There was a significant difference between the two sites in the stabilized frequency of IADFs in the different age classes (Fig. 3b). In the XE site, *A. unedo* formed a higher number of IADFs ($P \leq 0.001$) in growth rings from the last 5 yr (1–5 yr) compared with older growth rings. This phenomenon was not found in plants growing at the ME site. This statistical difference decreased in the other age classes (6–10 yr, $P \leq 0.01$; 16–20 yr, $P \leq 0.05$) as a result

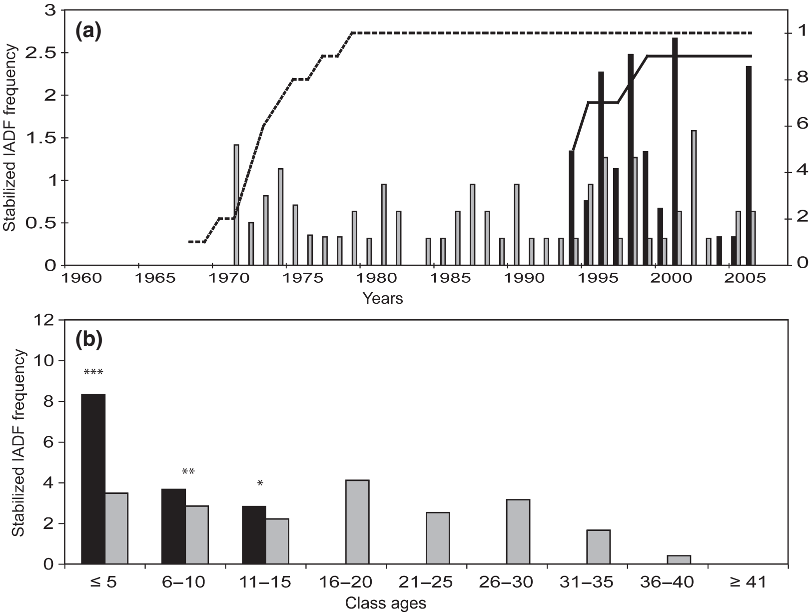

Fig. 3 (a) Stabilized intra-annual density fluctuation (IADF) frequencies in relation to calendar years of XE samples (black block) and ME samples (grey block). The number of trees at the ME (dot line) and XE (solid line) sites are shown. (b) Stabilized IADF frequencies in different age classes for trees at the XE (black block) and ME sites (grey block). Significance classes: *, $P < 0.05$, **, $P < 0.01$, ***, $P < 0.001$.

of a lower frequency of IADFs occurring at the XE site. The shrubs at the ME site had more IADFs in the middle age class (21–25 yr) than in the older age classes (> 30 yr).

For the common period of the two sites, the positions of the IADFs along the tree rings differed at the two sites: early- and middle-type IADFs were most frequent at the XE site (86%), while 89% of IADFs at the ME site were late-type. Occasionally, more than one type of IADF was observed in the same tree ring (Fig. 2d).

Spearmans' correlation coefficient between the chronologies of the stabilized IADF frequencies and the climate parameters (precipitation and temperature) was analysed from January to December of the current year (Table 1). At the XE site, IADFs were very frequent during the dry years ($r = -0.73$, $P < 0.001$). The IADF frequency was positively correlated with March and April temperatures ($r = 0.52$, $P < 0.01$). Trees at the ME site showed a positive correlation between the stabilized frequency of IADFs and the precipitation occurring in the June–September period ($r = 0.62$, $P < 0.01$). At the XE site, however, the relationship was, somewhat unexpectedly, the reverse. Air temperatures did not have a significant influence on the frequency of IADFs at the ME site.

Quantitative wood anatomy

Microphotographs of the cross-sections of *A. unedo* stems showed that its wood is diffuse-porous, characterized by rather many small vessels, with rounded to angular lumen. Vessels are mostly solitary, sometimes in rows or small groups in EW (Fig. 2). In the rings without IADFs, vessel size values varied along the ring following the usual trend, decreasing from EW to LW at both sites. The graph in Fig. 4 reports the simple moving average and nonlinear regression lines based on a sixth-order function for both rings with and without fluctuations from plants grown at the XE (panel a) and ME sites (panel b). At the XE site, rings with IADFs were characterized by a steeper decrease in vessel size, reaching a minimum at 50–60% ring width. Vessel size then increased again with higher measured values than in rings without fluctuations in the LW region. The variability between rings was lower in rings without fluctuations, which were also characterized by a higher correlation coefficient ($r^2 = 0.488$) when compared with the rings showing fluctuations ($r^2 = 0.399$). At the ME site, rings with IADFs were characterized by a progressive decrease in vessel size starting from EW, which was similar to that in rings without IADFs up to the 80% ring width. Afterwards, a sudden increase in vessel size was detectable. No steeper decrease in vessel size was found as compared with IADFs at the XE site, but a sudden increase in vessel lumen area was detectable. The variability between rings was lower in rings without IADFs, which were also characterized by a higher correlation coefficient ($r^2 = 0.503$) when compared with rings showing fluctuations ($r^2 = 0.384$).

Carbon isotopes

The $\delta^{13}C$ stable isotope annual chronologies are displayed in Fig. 5. The black line represents the average and SD of the shrubs growing at the XE site. The grey line is the average ± SD of the plants sampled at the ME site. $\delta^{13}C$ was consistently higher at the XE site, with a peak in 2002 and a significant difference ($P < 0.01$) between the two trends.

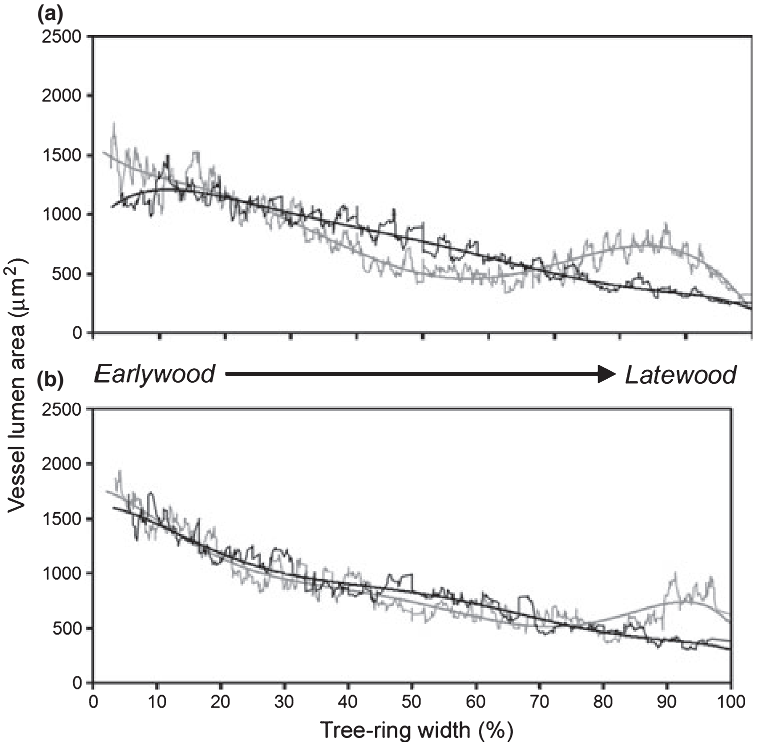

Fig. 4 Variation in vessel size along ring width in tree rings with intra-annual density fluctuations (IADFs, grey lines) and without IADFs (black lines) at the XE (a) and ME sites (b). Simple moving average and regression lines are reported for middle-IADFs at the XE site and late-IADFs at the ME site. Data are pooled from all analysed samples.

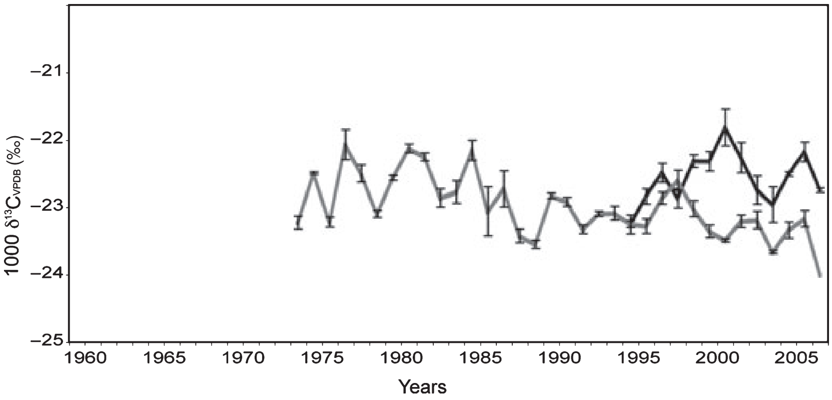

Fig. 5 Average δ^{13}C value ± standard deviation (SD) [‰] of the tree rings at the XE site (black line) and the ME site (grey line).

The carbon stable-isotope composition varied significantly during the season and a considerable annual fluctuation was observed in several tree rings from both site samples. In Fig. 6, the isotopic patterns are given for those years when most of the individuals presented IADFs and where the rings were sliced into EW, LW and IADF. At the XE site (Fig. 6a), the δ^{13}C values increased slightly at the beginning of the tree ring (EW), reached the highest value inside the IADFs and declined sharply in the last part of the ring (LW). δ^{13}C values were significantly different ($P < 0.01$) between the EW, LW and IADF in each section of the ring. Moreover, there was a difference between years, in particular for the IADFs, reaching the highest value of −21.33‰ during 2006.

At the ME site (Fig. 6b), the rings presented a contrasting seasonal trend of intra-annual δ^{13}C variations. The δ^{13}C values of EW and LW were comparable within the XE trees, but in all analysed rings the IADFs had a decrease in δ^{13}C.

The correlations between the seasonal patterns of δ^{13}C values of the IADFs were consistently different at the two sites (Table 1). At the XE site, the δ^{13}C of the IADFs correlated negatively with the April and May precipitation ($r = -0.44$, $P < 0.05$), while the EW values correlated positively with March and April temperatures ($r = 0.59$, $P < 0.001$) and negatively with precipitation ($r = -0.48$, $P < 0.01$). The LW data presented significant correlations with October temperatures ($r = 0.70$, $P < 0.001$) and June,

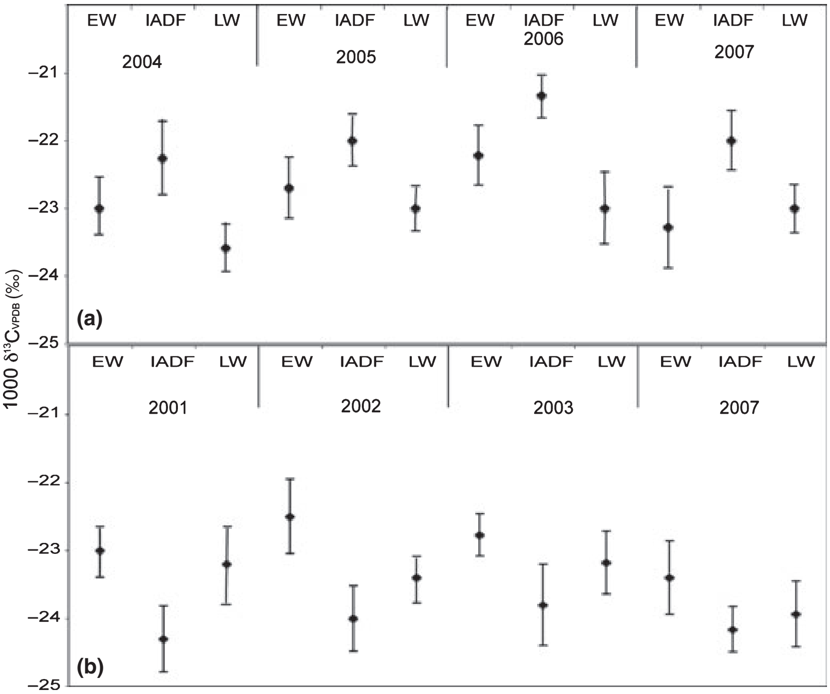

Fig. 6 Values of cellulose $\delta^{13}C \pm SD$ [‰] from different intra-annual sections: earlywood (EW), intra-annual density fluctuations (IADFs) and latewood (LW) at the XE site (a) and the ME site (b). In some years, the shrubs produced no IADFs. In such cases we selected different rings for the two sites.

July and August precipitation ($r = -0.74$, $P < 0.001$). At the ME site, precipitation influenced the $\delta^{13}C$ of IADFs significantly and positively (August and September, $r = 0.86$, $P < 0.001$). The correlations were negative for the EW values (March, April and May, $r = -0.78$, $P < 0.01$) and the LW values (August, September and October, $r = -0.98$, $P < 0.001$), while temperature never had a significant influence on the isotopic signal.

Fig. 7 shows the temporal changes in $\delta^{13}C$ over 4 yr according to the laser ablation–combustion line. With this method, the spatial and temporal resolution are high and a quasi-continuous pattern of the carbon isotope signal is

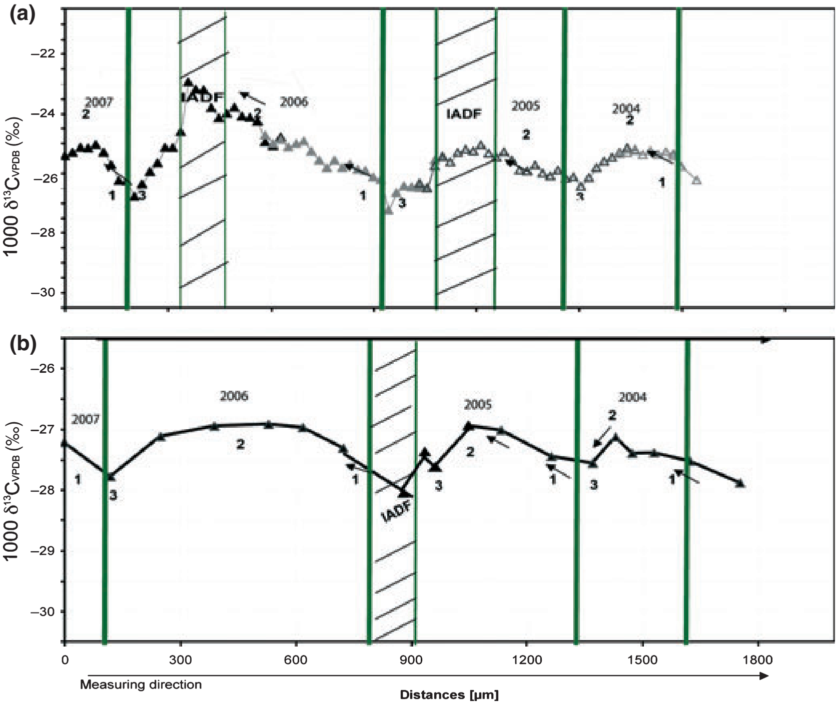

Fig. 7 Example of an isotopic measurement at the XE site (a) and the ME site (b). The numbers are given in per mill units (‰). The trend shows the typical seasonal tree-ring $\delta^{13}C$ pattern in each ring (see text for details). The green vertical lines indicate each tree-ring border. The intra-annual density fluctuations (IADFs) are identified. The colours indicate the different shooting days.

obtained. The figures refer to data from two samples, one from the XE site (Fig. 7a) and the other from the ME site (Fig. 7b). In all rings from both sites, the carbon isotope pattern can be divided into three sections (Helle & Schleser, 2004). The IADFs could be easily identified, even though they occurred at different locations in the rings and had different isotopic signals at the two sites. In the first section of each ring ('1' in the figure), that is, at the beginning of the growing season, the $\delta^{13}C$ values increased and reached an elevated value in the EW ('2'). In the latewood ('3'), $\delta^{13}C$ always reached a minimum value. The IADFs showed a maximum $\delta^{13}C$ value in the XE samples (Fig. 7a) and a minimum value at the ME site (Fig. 7b), confirming the results of the three slices analysed with the bulk isotope analysis described earlier. The $\delta^{13}C$ minima and maxima of consecutive years were very different, indicating intra-annual variability.

Soil samples

The mean value of the WHC and the mean value of the relative humidity in the top 10 cm of the ME soil were much higher (80.6 ± 18.9 and 3 ± 1%, respectively) than the corresponding values from the XE site (47.4 ± 14.2 and 17.1 + 0.9%). Those findings strengthened the occurrence of different water availability in the two sites. The soils at both sites were characterized as Eutric Cambisol (brown soil), coming from acid granite parent material (Frisch *et al.*, 2008) with a slightly acidic pH (6.2 ± 0.5).

Discussion

Arbutus unedo plants at the ME site had lower mean ring widths than those growing at the XE site. This phenomenon can be misleading considering that environmental conditions at the XE site were less favourable than those at the ME site, where the soil had a higher WHC. However, the size of the trees at both sites was comparable. Consequently, the reasons for the difference in tree-ring growth must arise from other factors, for example, tree age or a disturbance. At the XE site, all trees were younger than those located at the ME site and most of them showed signs of fires. Indeed, fires occurring at the XE site would have reduced competition between trees, created open spaces and released nutrients for the surviving plants. Moreover, since *A. unedo* is a resprouter species (Mesléard & Lepart, 1989; Bond & Midgley, 2001), the above-ground system that developed after the fires may have been grown faster using reserves from the old root system.

Mean sensitivity, which is a measure of the relative difference in ring width between two consecutive rings, increases with greater water stress (Fritts *et al.*, 1965). The mean sensitivity of trees at the XE site was higher than those of the mesic trees, even if the difference is not significant. This finding is in agreement with trends found by other authors in *Cedrus atlantica*, *Pinus sylvestris*, *Abies alba* and *Picea abies* (Till, 1987; Rigling *et al.*, 2002; Battipaglia *et al.*, 2009).

At the XE site, the negative correlation between ring width and April and May temperatures indicated that cambial activity was limited by high temperatures that worsen water deficit, since high temperatures are responsible for the increase of evapotranspiration and soil water losses (Rozas, 2005). The positive relation with the March and September temperatures reflects the importance of mild temperatures in those months, which are likely associated with higher water availability for plants. The lack of a relationship between precipitation and ring width at the XE site might indicate that, in such an environment, rainfall is never enough to compensate for soil water losses and to foster cell development (Antonova & Stasova, 1997; Deslauriers & Morin, 2005). At the ME site, both March temperatures and summer precipitation had a positive effect on tree-ring growth. Previous studies have demonstrated that the activity of cambial cells is highly responsive to temperature (Deslauriers & Morin, 2005; Zweifel *et al.*, 2006; Gričar *et al.*, 2007), especially when it increases during spring time (Keyser *et al.*, 2000).

The analysis of IADFs in *A. unedo* tree rings improved the resolution of climatic signals within the growing season. In fact, IADFs are generally produced in response to physiological, genetic control and to climate factors (Larson, 1960; Wimmer, 2002).

In our study, the higher stabilized IADF frequency in younger vs older trees at both sites might indicate that trees in the juvenile phase are more sensitive to environmental conditions and more prone to form IADFs than older plants. This is supported by other studies in which various species were analysed and more than one flush was observed (Rigling *et al.*, 2001; Copenheaver *et al.*, 2006; Vieira *et al.*, 2009). Similar age-dependent responses have been attributed to the longer growing season of young trees and their faster response to environmental changes (Villalba & Veblen, 1994; Rossi *et al.*, 2008). Indeed, some anatomical attributes (e.g. porosity, type of xylem elements) can be considered stable, while other traits (e.g. cell size) are more variable between juvenile and mature wood; this might explain the different hydraulic properties and sensitivity of the two wood types to environmental changes (De Micco *et al.*, 2008). Root systems can also play an important role, since older trees have deeper roots and are thus able to reach deeper water sources in the soil. In *A. unedo* trees, flushes seemed to produce multiple phases of growth, particularly in young individuals, and produced a large number of IADFs during the first 5 yr. This was especially marked at the XE site where the triggering factors (e.g. temperature and precipitation) were especially severe and limiting.

The position of IADFs in different species has been related to changes in climatic conditions, especially different degrees of drought, at different times of the growing season (Kuo & McGinnes, 1973; Campelo *et al.*, 2007). Our data could potentially be used to accurately pinpoint the timing of growth in relation to climatic and site changes. *A. unedo* trees growing at the XE site presented IADFs mainly at the beginning or in the middle of rings, which were related to lower annual total precipitation. The relationship between water deficit and occurrence of IADFs across EW has been observed in various coniferous species of the Mediterranean area (Campelo *et al.*, 2007; De Micco *et al.*, 2007). It is thought that decreasing precipitation is responsible for the formation of cells with increased wall thickness and reduced tracheid diameter. These cells become larger again and develop thinner walls under wetter climatic conditions (Fritts, 1976). This was also the case with the *A. unedo* trees growing at the XE site. From a functional point of view, the narrower vessels in IADFs that are formed during drought periods make the specific portion of wood less efficient in water conduction but safer since they reduce the risk of embolism (Tyree & Sperry, 1989; Sperry *et al.*, 2006). In these conditions, a slow water flow resulting from narrower vessels would accompany water transport resulting from vasicentric tracheids, since the contribution of different anatomical traits is additive (Carlquist, 1989).

In the *A. unedo* growing at the XE site, temperature did not appear to be as important as precipitation for the frequency of IADF formation, as only a correlation with March and April temperatures was observed. In 2002 and 2003, when the summer was extremely warm (Luterbacher *et al.*, 2004), we did not find any IADFs and the ring width was extremely narrow. Our hypothesis is that the water was so limited and the heat wave so strong that the plants reduced their cambial activity and the formation of new structures merely in order to survive. Under these conditions, growth never flushed again and no IADFs were formed. Cherubini *et al.* (2003) reported that, during dry years, *A. unedo* strongly reduces its hydraulic conductivity and photosynthetic activity. During summer the cambial activity may be strongly reduced or stop completely, especially in the plants with a shallow root system that does not allow them to endure the drought stress. Here, the XE site was also characterized by a relatively low WHC, which reaches a saturation point much sooner than soils with a higher WHC. Once a soil becomes saturated with water, all of the excess water and some of the nutrients that are in the soil solution are leached downward in the soil profile (Marano, 1989; Nannipieri, 1993). Consequently, nutrients are less available during periods of critical water stress, especially for young trees with a shallow root system (Baddeley & Watson, 2005).

At the ME site, IADFs were mainly located in the last part of the rings (late-IADFs) and were positively correlated with the precipitation from June to September period. The frequency of IADFs increased when precipitation amounts were higher, which suggests that the formation of fluctuations in the ME site could be triggered by principles different from those acting during dry conditions. In mesic conditions, the high formation of late-IADFs would be induced by rain events. When, in late summer, precipitation is higher than usual, the cambium dormancy resulting from water stress can be interrupted and new cells produced (Masiokas & Villalba, 2004). Anatomical investigations showed that late-IADFs in *A. unedo* were characterized by a clear increase in vessel size, which may confirm the sudden occurrence of precipitation events, because vessel diameter generally enlarges when water availability increases (Carlquist, 1966). In Mediterranean plants, vessel size is directly linked to theoretical hydraulic conductance per leaf area unit, which consequently increases under mesic conditions (Villar-Salvador *et al.*, 1997).

The double mechanism that triggers the formation of IADFs at the two sites was supported by QWA, which allowed vessel size to be measured and compared at the two sites. It was also confirmed by the observation of isotopic signals with the two methods. The $\delta^{13}C$ values obtained through the laser-ablation system represented the isotope ratios of natural wood, including lignin, while the $\delta^{13}C$ measured with the IRMS system was related to the extracted cellulose. Previous studies have shown an offset between the $\delta^{13}C$ of natural wood and cellulose that is constant and independent of season (Livingston & Spittlehouse, 1996; Borella *et al.*, 1998; Leuenberger *et al.*, 1998; Loader *et al.*, 2003; Eglin *et al.*, 2008). Schulze *et al.*'s (2004) comparison between the conventional method (elemental analysis and IRMS) and laser ablation indicated that the LA-C-GC_IRMS measurements are highly accurate. This high-resolution method allowed us to obtain intra-annual information on the content of $\delta^{13}C$, which is essential to understand the ecophysiological intra-annual processes (transpiration and photosynthesis) and the effect of water availability and water-use efficiency on *A. unedo* at the two sites. The $^{13}C : ^{12}C$ ratio can be directly related to carbon isotope discrimination, which provides an integrated record of the ratio of the intercellular to the atmospheric concentration of CO_2 ($c_i : c_a$) during the period in which the carbon was fixed. This ratio reflects the balance between assimilation rate and stomatal conductance (intrinsic water use efficiency, WUE_i), and thus is an indicator of the internal regulation of carbon uptake and water losses (Osmond *et al.*, 1980; Peñuelas & Azcón-Bieto, 1992; Duquesnay *et al.*, 1998; Arneth *et al.*, 2002; Saurer *et al.*, 2004).

In *A. unedo*, the annual $\delta^{13}C$ trend was always higher for trees growing at the XE site than for those at the ME site. This suggests that WUE_i is improved, under xeric conditions, probably because it is associated with lower stomatal conductance. The effect was particularly strong during some years, such as 2002 and 2003, and previous findings have also shown a robust increase in WUE_i as an adaptation to maintain a positive carbon balance during drought (Cowan & Farquhar, 1977; Raven, 2002; Galmes *et al.*, 2007). Under dry conditions, high WUE$_i$ in *A. unedo* would also be consistent with the occurrence of narrow vessels in IADFs, which, together with vasicentric tracheids, allow a slow but continuous water transport without deactivating the conduits as a result of embolism. In contrast, there was only a slight increase or even no change in WUE$_i$ at the ME site, as the δ^{13}C values measured during dry years indicate. This suggests that the response of stomatal conductance to soil water content is elastic. The lack of significant effects of drought treatment on WUE$_i$ in some Mediterranean species has been ascribed either to a proportional change in A_{max} (maximum carbon assimilation rate) and g_s (stomatal conductance) or to a parallel increase in stomatal and nonstomatal limitations (Ripullone *et al.*, 2009). The seasonal change in δ^{13}C in different compartments of the wood provides additional information about wood development and the environmental, climatic influences on it and interaction with carbohydrate storage (Gleixner *et al.*, 1993; Gessler *et al.*, 2009). Heavy δ^{13}C values in EW reflect mobilization of reserves at the beginning of the vegetation period (Helle & Schleser, 2004; Vaganov *et al.*, 2009), while the isotopic value of LW is strongly influenced by climatic signals (Jäggi *et al.*, 2002). De Micco *et al.* (2007), in their study on *P. pinaster*, showed that the IADF δ^{13}C was consistently heavier than LW δ^{13}C, indicating an appreciable closure of stomata to save water. A similar trend was found in *A. unedo* trees growing at the XE site, which also indicates that stomata were closed, as does the position of IADFs. Negative correlations between precipitation and δ^{13}C of IADFs confirmed that, when precipitation decreases, the stomata respond to the resulting water limitation by reducing conductance. Consequently, the discrimination against ^{13}C decreases and δ^{13}C increase. The lack of a significant correlation between δ^{13}C of IADFs and temperature is consistent with earlier findings (Saurer *et al.*, 1995, 1997; Cullen & Grierson, 2007; Battipaglia *et al.*, 2009), where water conditions appeared to explain the carbon isotope variation in many species better than temperature, at least at dry sites.

At the ME site, the seasonal δ^{13}C presented, surprisingly, δ^{13}C in IADFs that was lighter than that in EW and, during some years, even lighter than in LW. The positive correlation between δ^{13}C in IADFs and precipitation confirmed that the formation of IADFs at this site was linked with the regrowth of the rings in the last part of the growing season after rain events. *A. unedo* responses to drought seem to be strongly mediated by the depth of the root system in comparison with other species and to depend on how long water remains in the upper soil layers (Mereu *et al.*, 2009). The high correlations between δ^{13}C in EW and LW and precipitation during the whole growing season confirm the importance of the presence of water and the capacity of *A. unedo* to react to sudden favourable environmental conditions.

The different position and characteristics of IADFs in the rings support the hypothesis that this Mediterranean species is very plastic in coping with seasonal water deficits under different site conditions as it has efficient mechanisms of stomatal closure (Aussenac & Valette, 1982; Acherar *et al.*, 1991).

In conclusion, the overall analysis indicated that *A. unedo* wood has a high plasticity, which should make this species capable of withstanding the water stress conditions typically associated with Mediterranean-type ecosystems, and also able to cope with future changes in rainfall patterns (IPCC, 2007).

We obtained detailed information on the impact of climatic conditions on wood growth at the seasonal level by combining classical dendrochronology with isotopic analysis and QWA. Identifying trends in the variation in vessel size and δ^{13}C has been helpful in pinpointing IADFs and tree-ring boundaries. In particular, the LA-C-GC_IRMS technique proved to be very useful for dating the samples, since the isotopic pattern presented a clear synchronization with the ring borders and allowed false rings to be distinguished from true EW-LW formation. This multidisciplinary approach is valuable to achieve representation with small sample size, thus overcoming the limitations found in the Mediterranean environments where it is difficult to find good representative samples. It should be applied in the analysis of other species, to determine whether they are affected in a similar way by drought at the intra-annual level.

Acknowledgements

We thank I. Schaefer, L. Nardella, D. Giove, F. Vaccari, M. Nötzli, W. Schoch and H. Gärtner for assistance during this research and Dr. S. Dingwall Stucki for the language revision.

References

Acherar M, Rambal S, Lepart J. 1991. Évolution du potentiel hydrique foliaire et de la conductance stomatique de quatrechênes méditerranéens lors d'une période de desséchement. *Annals of Forest Science* **48**: 561–573.

Antonova G, Stasova V. 1997. Effects of environmental factors on wood formation in larch (*Larix sibirica* Ldb.) stems. *Trees (Berlin)* **11**: 462–468.

Arneth A, Lloyd J, Santruckova H, Bird M, Grigoryev S, Kalaschni-kov YN, Gleixner G, Schulze ED. 2002. Response of central Siberian Scots pine to soil water deficit and long-term trends in atmospheric CO$_2$ concentration. *Global Biogeochemical Cycles* **16**: 1005.

Aussenac C, Valette JC. 1982. Comportement hydrique estival de *Cedrus atlantica* Manetti, *Quercus ilex* L. et *Quercus puberscens* Will et de divers pins dans le Mont Ventoux. *Annals of Forest Science* **39**: 41–62.

Baas P. 1976. Some functional and adaptative aspects of vessel members morphology. In: Baas P, Bolton AJ, Catling DM, eds. *Wood structure in* *biological and technological research*. Leiden Bot. Series 3. The Hague, The Netherlands: Leiden University, 157–181.

Baas P, Ewers FW, Davis SD, Wheeler EA. 2004. Evolution of xylem physiology. In: Hemsley A, Poole I, eds. *The evolution of plant physiology*. Amsterdam, The Netherlands: Elsevier Scientific, 273–295.

Baddeley J, Watson CA. 2005. Influence of root diameter, tree age, soil depth and season on fine root survivorship in *Prunus avium*. *Plant and Soil* **276**: 15–22.

Battipaglia G, Jäggi M, Saurer M, Siegwolf RTW, Cotrufo MF. 2008. Climatic sensitivity of δ^{18}O in the wood and cellulose of tree rings: results from a mixed stand of *Acer pseudoplatanus* L. and *Fagus sylvatica*. *Palaeogeography Palaeoclimatology Palaeoecology* **261**: 193–202.

Battipaglia G, Saurer M, Cherubini P, Siegwolf RTW, Cotrufo MF. 2009. Tree rings indicate different drought resistance of a native (*Abies alba* Mill.) and a nonnative (*Picea abies* L. Karst.) species co-occurring at a dry site in Southern Italy. *Forest Ecology and Management* **25**: 820–828.

Bond WJ, Midgley JJ. 2001. Ecology of sprouting in woody plants: the persistence niche. *Trends in Ecology and Evolution* **16**: 45–51.

Borella S, Leuenberger M, Saurer M, Siegwolf TRW. 1998. Reducing uncertainties in δ^{13}C analysis of tree rings: poolings, milling and cellulose extraction. *Journal of Geophysical Research* **103**: 19519–19526.

Campelo F, Nabais C, Freitas H, Gutiérrez E. 2007. Climatic significance of tree-ring width and intra-annual density fluctuations in *Pinus pinea* from a dry Mediterranean area in Portugal. *Annals of Forest Science* **64**: 229–238.

Carlquist S. 1966. Wood anatomy of Compositae: a summary, with comments on factors controlling wood evolution. *Aliso* **6**: 25–44.

Carlquist S. 1975. *Ecological strategies of xylem evolution*. Berkeley, CA, USA: University of California Press.

Carlquist S. 1989. Adaptive wood anatomy of chaparral shrubs. In: Keely JE, ed. *The California chaparral: paradigms re-examined*. Los Angeles, CA, USA: Los Angeles Country Museum of Natural History Contributions, 25–35.

Cherubini P, Gartner BL, Tognetti R, Bräker OU, Schoch W, Innes JL. 2003. Identification, measurement and interpretation of tree rings in woody species from mediterranean climates. *Biological Reviews of the Cambridge Philosophical Society* **78**: 119–148.

Copenheaver CA, Pokorski EA, Currie JE, Abrams MD. 2006. Causation of false ring formation in *Pinus banksiana*: a comparison of age, canopy class, climate, and growth rate. *Forest Ecology and Management* **236**: 348–355.

Correia O, Catarino F, Tenhunen JD, Lange OL. 1987. Regulation of water use by four species of Cistus in the scrub vegetation of the Serra de Arrabida, Portugal. In: Tenhunen JD, Catarino FM, Lange OL, Oechel WC, eds. *Plant response to stress: functional analysis in Mediterranean ecosystems*. NATO ASI series. Berlin, Germany: Springer, 247–258.

Cowan IR, Farquhar GD. 1977. Stomatal function in relation to leaf metabolism and environment. *Symposia of the Society for Experimental Biology* **31**: 471–505.

Cullen LE, Grierson PF. 2007. A stable oxygen, but not carbon, isotope chronology of *Callitris columellaris* reflects recent climate change in north-western Australia. *Climatic Change* **85**: 213–229.

De Micco V, Aronne G, Baas P. 2008. Wood anatomy and hydraulic architecture of stems and twigs of some Mediterranean trees and shrubs along a mesic-xeric gradient. *Trees (Berlin)* **22**: 643–655.

De Micco V, Aronne G, Toraldo G. 2006. Method to classify xylem cell types using cross sections of 1-year-old branches in Mediterranean woody species. *Trees* **20**: 474–482.

De Micco V, Saurer M, Aronne G, Tognetti R, Cherubini P. 2007. Variations of wood anatomy and δ^{13}C within-tree rings of coastal *Pinus pinaster* showing intraannual density fluctuations. *International Association of Wood Anatomists Journal* **28**: 61–74.

Deslauriers A, Morin H. 2005. Intra-annual tracheid production in balsam fir stems and the effect of meteorological variables. *Trees* **19**: 402–408.

Duquesnay A, Breda N, Stievenard M, Dupouey JL. 1998. Changes of tree-ring δ^{13}C and water-use efficiency of beech (*Fagus sylvatica* L.) in north-eastern France during the past century. *Plant, Cell & Environment* **21**: 565–572.

Eglin T, Maunoury-Danger F, Fresnau C, Lelarge C, Pollet B, Lapierre C, Francois C, Damesin C. 2008. Biochemical composition is not the main factor influencing variability in carbon isotope composition of tree rings. *Tree Physiology* **28**: 1619–1629.

Farquhar GD, Richards RA. 1984. Isotopic composition of plant carbon correlates with water use efficiency of wheat genotypes. *Australian Journal of Plant Physiology* **11**: 539–552.

Francey RJ, Allison CE, Etheridge DM, Trudinger CM, Enting IG, Leuenberger M, Langenfeld RL, Michel E, Steele LP. 1999. A 1000-year high precision record of δ13C in atmospheric CO$_2$. *Tellus* **51**: 170–193.

Frisch W, Meschede M, Kuhlemann J. 2008. *Elba: Geologie, Struktur, Exkursionen und Natur*. Berlin, Germany: Gebrüder Borntraeger.

Fritts HC. 1976. *Tree rings and climate*. London, UK: Academic Press.

Fritts HC, Smith DG, Cardis JW, Budelsky CA. 1965. Tree-ring characteristics along a vegetation gradient in northern Arizona. *Ecology* **46**: 393–401.

Galmes J, Medrano H, Flexas J. 2007. Photosynthetic limitations in response to water stress and recovery in Mediterranean plants with different growth forms. *New Phytologist* **175**: 81–93. doi: 10.1111/j.1469-8137.2007.02087.x

Gärtner H, Schweingruber FH, Dikau R. 2001. Determination of erosion rates by analyzing structural changes in the growth pattern of exposed roots. *Dendrochronologia* **19**: 81–91.

Gessler A, Brandes E, Buchmann N, Helle G, Rennenberg H, Barnard RL. 2009. Tracing carbon and oxygen isotope signals from newly assimilated sugars in the leaves to the tree ring archive. *Plant, Cell & Environment* **32**: 780–795.

Gleixner G, Danier HJ, Werner RA, Schmidt HL. 1993. Correlation between the ^{13}C content of primary and secondary plant products in different cell compartments and that in decomposing basidiomycetes. *Plant Physiology* **102**: 1287–1290.

Glerum C. 1970. Drought ring formation in conifers. *Forest Science* **16**: 246–248.

Gričar J, Zupancic M, Cufar K, Oven P. 2007. Regular cambial activity and xylem and floem formation in locally heated and cooled stem portions of Norway spruce. *Wood Science and Technology* **41**: 463–475.

Helle G, Schleser H. 2004. Beyond CO$_2$-fixation by Rubisco- an interpretation of ^{13}C/^{12}C variations in tree rings from novel intra-seasonal studies on broad-leaf trees. *Plant, Cell & Environment* **27**: 367–380.

Holmes RL. 1983. Computer-assisted quality control in tree-ring dating and measurement. *Tree-Ring Bulletin* **43**: 68–78.

Intergovernmental Panel on Climate Change (IPCC). 2007. *Climate change 2007: mitigation. Contribution of working group III to the fourth assessment report of the intergovernmental panel on climate change*. Cambridge, UK: Cambridge University Press.

Jacobsen AL, Agenbag L, Esler KJ, Pratt RB, Ewers FW, Davis SD. 2007a. Xylem density, biomechanics, and anatomical traits correlate with water stress in 17 evergreen shrub species of the Mediterranean-type climate region of South Africa. *Journal of Ecology* **95**: 171–183.

Jacobsen AL, Pratt RB, Ewers FW, Davis SD. 2007b. Cavitation resistance among 26 chaparral species of southern California. *Ecological Monographs* **77**: 99–115.

Jäggi M, Saurer M, Fuhrer J, Siegwolf TRW. 2002. The relationship between the stable carbon isotope composition of needle bulk material, starch, and tree rings in *Picea abies*. *Oecologia* **131**: 325–332.

Keyser AR, Kimball JS, Nemani RR, Running SW. 2000. Simulating the effects of climate change on the carbon balance of North American high-latitude forests. *Global Change Biology* **6**: 185–195.

Kuo ML, McGinnes EA Jr. 1973. Variation of anatomical structure of false rings in Eastern red cedar. *Wood Science* **5**: 205–210.

Larson PR. 1960. A physiological consideration of the springwood-summerwood transition in red pine. *Forest Science* **6**: 110–122.

Leuenberger M, Borella S, Stocker T, Saurer M, Siegwolf R, Schweingruber F, Matyssek R. 1998. Stable isotopes in tree rings as climate and stress indicators. In: *Final Report* NRP 31. Vdf Hochschulverl. an der ETH, Zürich, 200.

Livingston NJ, Spittlehouse DL. 1996. Carbon isotope fractionation in tree ring early- and latewood in relation to intra-growing season water balance. *Plant, Cell & Environment* **19**: 768–774.

Loader NJ, Robertson I, McCarroll D. 2003. Comparison of stable carbon isotope ratios in the whole wood, cellulose and lignin of oak tree-rings. *Paleogeography Paleoclimatology Palaeoecology* **196**: 395–407.

Luterbacher J, Dietrich D, Xoplaki E, Grosjean M, Wanner H. 2004. European seasonal and annual temperature variability, trends and extremes since 1500 A.D. *Science* **303**: 1499–1503.

Maltez-Mouro S, Garcia LV, Maranon T, Freitas H. 2007. Recruitment patterns in a Mediterranean oak forest: a case study showing the importance of the spatial component. *Forest Science* **53**: 645–652.

Marano B. 1989. *La fertilità del suolo e nutrizione delle piante*. Livorno, Italy: Edizioni Nannipieri.

Margaris NS, Papadogianni P. 1977. Cambial activity in some plants dominating phryganic formations in Greece. *Phyton (Greece)* **36**: 1–5.

Masiokas M, Villalba R. 2004. Climatic significance of intra-annual bands in the wood of *Nothofagus pumilio* in southern Patagonia. *Trees (Berlin)* **18**: 696–704.

Matzner SL, Rice KJ, Richards JH. 2001. Factors affecting the relationship between carbon isotope discrimination and transpiration efficiency in blue oak (*Quercus douglasii*). *Australian Journal of Plant Physiology* **28**: 49–56.

McCarroll D, Loader NJ. 2004. Stable isotope is tree rings. *Quaternary Science Reviews* **23**: 771–801.

Mereu S, Salvatori E, Fusaro L, Gerosa G, Muys B, Manes F. 2009. An integrated approach shows different use of water resources from Mediterranean maquis species in a coastal dune ecosystem. *Biogeosciences* **6**: 2599–2610.

Mesléard F, Lepart J. 1989. Continuous basal sprouting from a lignotuber: *Arbutus unedo* L. And *Erica arborea* L., as woody Mediterranean examples. *Oecologia* **80**: 127–131.

Nannipieri P. 1993. *Ciclo della sostanza organica nel suolo*. Bologna, Italy: Pàtron Editore.

Ogaya R, Peñuelas J. 2008. Changes in leaf δ^{13}C and δ^{15}N for three Mediterranean tree species in relation to soil water availability. *Acta Oecologia* **34**: 331–338.

Osborn TJ, Briffa KR, Jones PD. 1997. Adjusting variance for sample size in tree-ring chronologies and other regional mean time series. *Dendrochronologia* **15**: 89–99.

Osmond CB, Bjorkman O, Anderson DJ. 1980. *Physiological processes in plant ecology*. New York, NY, USA: Springer.

Panek JA. 1996. Correlations between stable carbon-isotope abundance and hydraulic conductivity in Douglas-fir across a climate gradient in Oregon, USA. *Tree Physiology* **16**: 747–755.

Panek JA, Goldstein AH. 2001. Response of stomatal conductance to drought in ponderosa pine: implications for carbon and ozone uptake. *Tree physiology* **21**: 337–344.

Peñuelas J. 1996. Overview on current and past global change in the Mediterranean ecosystems. *Orsis* **11**: 165–175.

Peñuelas J, Azcón-Bieto J. 1992. Changes in leaf Δ^{13}C of herbarium plant species during the last 3 centuries of CO_2 increase. *Plant, Cell & Environment* **15**: 485–489.

Ponton S, Dupouey JL, Breda N, Feuillat F, Bodenes C, Dreyer E. 2001. Carbon isotope discrimination and wood anatomy variations in mixed stands of *Quercus robur* and *Quercus petraea*. *Plant, Cell & Environment* **24**: 861–868.

Raven JA. 2002. Selection pressures on stomatal evolution. *New Phytologist* **153**: 371–386.

Rigling A, Bräker O, Schneiter G, Schweingruber F. 2002. Intra-annual tree-ring parameters indicating differences in drought stress of *Pinus sylvestris* forests within the Erico-Pinion in the Valais (Switzerland). *Plant Ecology* **163**: 105–121.

Rigling A, Waldner PO, Forster T, Bräker O, Pouttu A. 2001. Ecological interpretation of tree-ring width and intraannual density fluctuations in *Pinus sylvestris* on dry sites in the central Alps and Siberia. *Canadian Journal of Forest Research* **31**: 18–31.

Ripullone F, Borghetti M, Raddi S, Vicinelli E, Baraldi R, Guerrieri MR, Nolé A, Magnani F. 2009. Physiological and structural changes in response to altered precipitation regimes in a Mediterranean macchia ecosystem. *Trees* **28**: 823–834.

Rossi S, Deslauriers A, Anfodillo T, Carrer M. 2008. Age-dependent xylogenesis in timberline conifers. *New Phytologist* **177**: 199–208.

Rozas V. 2005. Dendrochronology of pedunculate oak (*Quercus robur* L.) in an old-growth pollarded woodland in northern Spain: tree ring growth responses to climate. *Annals of forest Science* **62**: 209–218.

Rundel PW. 1991. Shrub life forms. In: Mooney HA, Winner WE, Pell EJ, Chu E, eds. *Responses of plants to multiple stresses*. New York, NY, USA: Academic Press, 345–370.

Salleo S, Nardini A, Lo Gullo MA. 1997. Is sclerophylly of Mediterranean evergreens an adaptation to drought? *New Phytologist* **135**: 603–612.

Saurer M, Borella S, Schweingruber F, Siegwolf R. 1997. Stable carbon isotopes in tree rings of beech: climatic versus site-related influences. *Trees* **11**: 291–297.

Saurer M, Siegenthaler IU, Schweingruber F. 1995. The climate carbon isotope ratios in tree ring and the significance in site condition. *Tellus* **47B**: 320–330.

Saurer M, Siegwolf RTW, Schweingruber FH. 2004. Carbon isotope discrimination indicates improving water-use efficiency of trees in northern Eurasia over the last 100 years. *Global Change Biology* **10**: 2109–2120.

Scheidegger Y, Saurer M, Bahn M, Siegwolf R. 2000. Linking stable oxygen and carbon isotopes with stomatal conductance and photosynthetic capacity: a conceptual model. *Oecologia* **125**: 350–357.

Schulman E. 1938. Classification of false annual rings in Monterey pine. *Tree-ring Bulletin* **4**: 4–7.

Schulze B, Wirth C, Linke P, Brand WA, Kuhlmann I, Horna V, Schulze ED. 2004. Laser-Ablation-Combustion-GC-IRMS— A new method for online analysis of intra-annual variation of δ^{13}C in tree-rings. *Tree Physiology* **24**: 1193–1201.

Schweingruber FH. 1978. *Mikroskopische holzanatomie*. Birmensdorf, Switzerland: Eidgenössische Anstalt für das forstliche Versuchswesen.

Sperry JS, Hacke UG, Pittermann J. 2006. Size and function in conifer tracheids and angiosperm vessels. *American Journal of Botany* **93**: 1490–1500.

Stokes MA, Smiley TL. 1968. *An introduction to tree-ring dating*. Chicago, IL, USA: University of Chicago.

Till C. 1987. The summary response function of *Cedrus atlantica* (endl.) carriere in Morocco. *Tree Bulletin* **47**: 23–36.

Tingley MA. 1937. Double growth rings in Red Astrachan. *Proceedings American Society Horticultural Science* **34**: 61.

Tyree MT, Sperry JS. 1989. Vulnerability of xylem to cavitation and embolism. *Annual Review of Plant Physiology and Plant Molecular Biology* **40**: 19–38.

USDA, Natural Resources Conservation Service, National Soil Survey Center. 1996. *Soil survey laboratory methods manual*. Soil Survey

Investigations Report No. 42, Version 3.0. Washington, DC, USA: U.S. Department Agriculture.

Vaganov EA, Schulze ED, Skomarkova MV, Knohl A, Brand WA, Roscher C. 2009. Intra-annual variability of anatomical structure and δ^{13}C values within tree rings of spruce and pine in alpine, temperate and boreal Europe. *Oecologia* **161**: 729–745.

Vieira J, Campelo F, Nabais C. 2009. Age-dependent responses of tree-ring growth and intra-annual density fluctuations of *Pinus pinaster* to Mediterranean climate. *Trees* **23**: 257–265.

Villalba R, Veblen TT. 1994. A tree-ring record of dry spring wet summer events in the forest-steppe ecotone northern Patagonia, Argentina. In: Dean JS, Meko DM, Swetnam TW, eds. *Tree rings environment and humanity*. Radiocarbon, Spec., Issue 107–116.

Villar-Salvador P, Castro-Diéz P, Pérez-Rontomé C, Montserrat-Martì G. 1997. Stem xylem features in three Quercus (Fagaceae) species along a climatic gradient in NE Spain. *Trees (Berlin)* **12**: 90–96.

Wigley TML, Briffa KR, Jones PD. 1984. On the average value of correlated time series with application in dendroclimatology and hydrometereology. *Journal of Climate and Applied Meteorology* **23**: 201–221.

Wilson BF. 1995. Shrub stems: form and function. In: Gartner BL, eds. *Plant stems: physiology and functional morphology*. San Diego, CA, USA: Academic Press, 91–102.

Wimmer R. 2002. Wood anatomical features in tree-rings as indicators of environmental change. *Dendrochronologia* **20**: 21–36.

Zweifel R, Zimmermann L, Zeuginand F, Newbery DM. 2006. Intra-annual radial growth and water relations of trees: implication towards a growth mechanism. *Journal of Experimental Botany* **57**: 1445–1459.